Corrosion Science xxx (2014) xxx–xxx

Contents lists available at ScienceDirect

Corrosion Science

journal homepage: www.elsevier.com/locate/corsci

Tracking the progression of bronze disease – A synchrotron X-ray diffraction study of nantokite hydrolysis

Rosie Grayburn [a,b], Mark Dowsett [a], Matthew Hand [a], Pieter-Jan Sabbe [b], Paul Thompson [c], Annemie Adriaens [b,*]

[a] Department of Physics, University of Warwick, Coventry CV4 7AL, UK
[b] Department of Analytical Chemistry, Ghent University, Krijgslaan 281 S12, B9000 Ghent, Belgium
[c] XMaS@ESRF, BP 220, 38043 Grenoble, France

ARTICLE INFO

Article history:
Received 19 May 2014
Accepted 12 November 2014
Available online xxxx

Keywords:
A. Copper
B. XRD

ABSTRACT

The hydrolysis of nantokite to form cuprite could be a reaction step in the progression of bronze disease on cupreous *objects d'art*. In this paper, this transformation is visualized for the first time using a time-resolved synchrotron X-ray diffraction experiment. Complete conversion of nantokite to cuprite was observed on a nantokite patina over 5 h in water using time-resolved synchrotron X-ray diffraction.

1. Introduction

Bronze disease is the catalytic corrosion of copper by reaction with oxygen, water and, most importantly, chloride ions [1]. In a marine or buried environment, chloride ions can react with copper to produce a layer of nantokite (CuCl) next to the metallic surface [2–5]. Once excavated, the nantokite layer is the starting point for bronze disease due to the changing environment namely elevated oxygen levels [6]. The visual effect of bronze disease is the eventual formation of bright green, powdery spots of copper trihydroxychlorides [7], which is also accompanied by stress cracking of the surface due to the volume change and subsequent deeper penetration of chlorides into the metal [8].

However, the chemical pathway to this powdery end-point is not wholly agreed upon. Nantokite is formed by reaction with chlorides (Eq. (1)) but the next step depends on the environmental conditions, especially the presence of water and oxygen. Although cuprite (Cu_2O) is usually thought to be passivating, it can react to form nantokite if chloride ions are still present (reverse Eq. (2)) and pH is lower than 5, thus proceeding to the irreversible trihydroxychloride [9].

Free energy calculations have been performed on some of the reactions known to take place during bronze disease corrosion. Scott calculated that the reaction of nantokite, oxygen and water to form trihydroxychlorides such as paratacamite ($Cu_2(OH)_3Cl$) (Eq. (1)) has a standard free energy of formation of −1510 kJ/mol [10]. The reaction between nantokite and water (Eq. (2)) would not take place due to a positive value of Standard Gibbs Free Energy of Reaction ($\Delta G_{react}{}^0$) of 56.5 kJ/mol.

$$4CuCl + O_2 + 4H_2O \rightarrow 2Cu_2(OH)_3Cl + 2HCl \quad (1)$$

$$2CuCl + H_2O \rightarrow Cu_2O + 2H^+ + 2Cl^- \quad (2)$$

While it is true that when using Standard Gibbs Free Energy of Formation values to calculate $\Delta G_{react}{}^0$ a positive value does result (+70.33 kJ mol^{-1} using ΔS^0, ΔH^0 and ΔG^0 values for all components of Eq. (2) [11]) it is also true that standard conditions do not necessarily apply to this reaction in context, i.e. 298 K, 1 mol, 1 bar. In addition, MacLeod stated that the reaction was at equilibrium at pH 5.2 after research determining the Pourbaix diagrams of the system was carried out by Bianchi and Longhi [12]. Dilution of this system to ensure high pH values means that the reaction can proceed to completion above pH 5.2. Pollard and co-workers found that despite the positive Gibbs Free Energy of Reaction the reaction of nantokite to cuprite does still proceed under most oxidizing conditions in a burial environment [13]. However, upon excavation and exposure to ambient conditions the main products will be copper trihydroxychlorides.

The production of nantokite has been studied previously [14]. In this work we aim to record the transformation of nantokite to cuprite in water for the first time using time-resolved synchrotron X-ray diffraction (SR-XRD) in an ambient environment.

* Corresponding author. Tel.: +32 9 264 4826.
E-mail address: annemie.adriaens@ugent.be (A. Adriaens).

http://dx.doi.org/10.1016/j.corsci.2014.11.021
0010-938X/

2. Experimental method

All SR-XRD data were collected using a MAR CCD 165 (Mar USA Inc. Evanston, IL, USA) 2D detector at XMaS (station BM28, ESRF, Grenoble, France). The camera was mounted at 45° to the incident X-ray beam. The starting coupon was imaged using a 1-s exposure time. Time-lapse sequences of images were collected, comprising XRD patterns with a 1-s exposure time recorded every 7 s for 2 h. A fast shutter was used to shield the sample from X-rays between exposures. When the sequence had finished, the coupon was soaked in water for 3 h then a further pattern (1-s exposure) captured a final image of the coupon. Data were batch processed using the code esaProject (© EVA Surface Analysis 2006–2012) [15] to integrate 1-D diffraction patterns from the rings, normalize them to the beam monitor, remove the background, and extract trends.

A copper coupon (Goodfellow, Cambridge UK, 99.9% purity) with a nantokite patina (prepared according to the Faltermeier procedure [16], approx. 100 μm thickness) was mounted on the working electrode within the eCell Mk IV (EVA Surface Analysis, UK) [17]. A 50 μL droplet of DI water (pH 6.95) was placed on the inside center of the Kapton® window using a micropipette and the window was mounted on the eCell. The time-lapse sequence was initiated as the coupon was raised into contact with the droplet by remote control. The liquid is sandwiched between the coupon surface and the window in a layer around 100 μm thick. The experiment was repeated on a fresh nantokite surface using a 1% sodium sesquicarbonate droplet (pH 9.9). The experimental setup is similar to that depicted in Fig. 2 of Ref. [14].

3. Results and discussion

Before exposing the nantokite patina to water, an SR-XRD image of the surface was collected. This confirmed the presence of nantokite on copper, but with a small amount of paratacamite contamination (Fig. 1). Paratacamite is likely to be a product of the nantokite patina oxidation in air during transportation to the beamline and shows that on exposure to air the nantokite patina is already transforming due to bronze disease. Paratacamite is soluble so must have dissolved away during exposure to water, and therefore plays no further role in the bronze disease process in this case.

Nantokite patinas were exposed to DI water and 1% sesquicarbonate droplets. Every hundredth pattern was plotted into a waterfall plot so that the change in peak intensity (and therefore surface concentration) over time can be viewed easily (Figs. 2 and 3). In terms of time, every 100th scan equates to a 13-min interval approximately.

Figs. 2 and 3 show that cuprite is formed in both neutral and basic droplets. Since no detectable cuprite is seen in the starting material (Fig. 1) we can deduce that cuprite growth happens as a direct result of contact with the droplet. As cuprite is growing without the presence of trihydroxychlorides such as paratacamite, it could be concluded that the *in situ* conditions in the eCell are providing a 'burial' environment (low oxygen, high water content) as opposed to an 'excavated' environment (higher oxygen content), therefore proving Pollard's hypothesis [13] that cuprite forms in burial conditions.

Over time, the areas under the cuprite reflections can be seen to be increasing, although the highest intensity peaks are still copper and nantokite. Figs. 2 and 3 show the nantokite peak unchanging over time while cuprite grows on the patina from exposure of

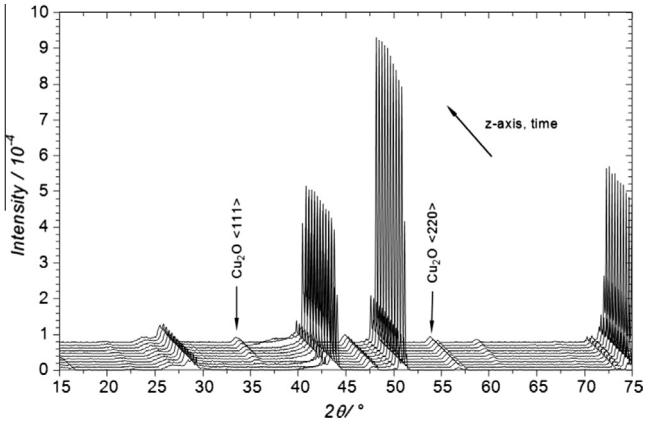

Fig. 2. A waterfall plot showing SR-XRD patterns of a nantokite patina in a DI water droplet (pH 6.95) over 8000 s ($z = 0$ is $t = 0$). Patterns are at 800 s intervals.

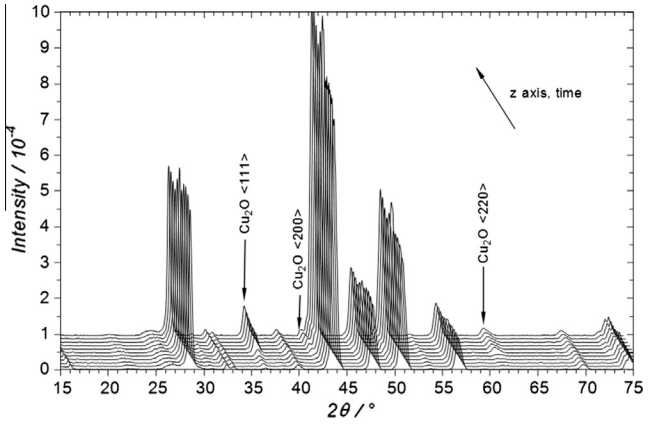

Fig. 3. A waterfall plot showing SR-XRD patterns of a nantokite patina in a 1% sesquicarbonate droplet (pH 9.9) over 8000 s ($z = 0$ is $t = 0$). Patterns are at 800 s intervals.

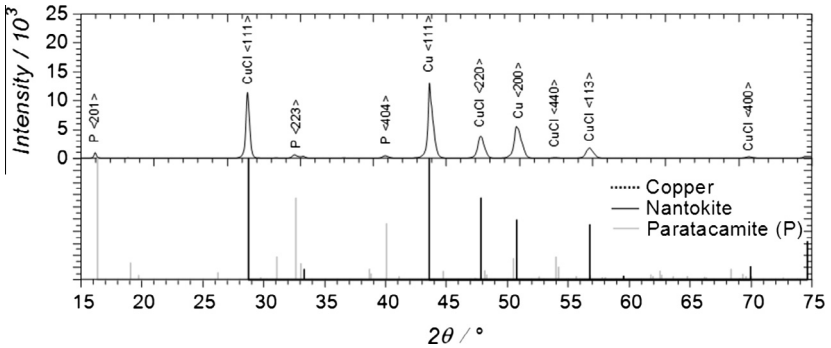

Fig. 1. SR-XRD pattern of nantokite on copper before water droplet exposure.

Please cite this article in press as: R. Grayburn et al., Tracking the progression of bronze disease – A synchrotron X-ray diffraction study of nantokite hydrolysis, Corros. Sci. (2014), http://dx.doi.org/10.1016/j.corsci.2014.11.021

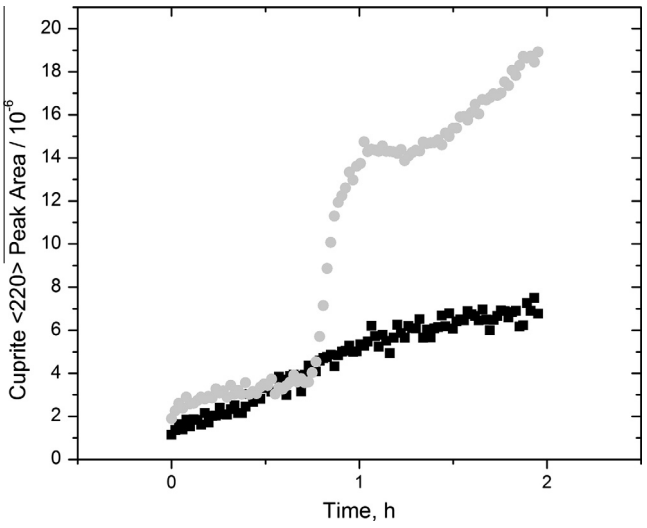

Fig. 4. Cuprite peak area vs acquisition time. Peak areas were extracted from under the ⟨220⟩ reflection water (black squares) and sodium sesquicarbonate (gray circles) datasets.

the nantokite to water. The zero rate of change over time of nantokite could be due to further corrosion of the copper coupon to nantokite, thus keeping the nantokite in steady state. This could be caused by the release of chloride ions from the reaction of nantokite with water (Eq. (2)). These ions could penetrate the nantokite layer and react with further copper metal to regenerate nantokite:

$$Cu + Cl^- \rightarrow CuCl + e^- \quad (3)$$

Additionally, the presence of Cl^- ions near the copper metal could originate from the patina preparation since the protocol for nantokite patina formation involves soaking the coupon in 1 M $CuCl_2$ solution for 1 day [16]. This result demonstrates the catalytic nature of the system.

The peak areas from the datasets can be extracted and plotted against acquisition time (Fig. 4). In this way, the change in cuprite peak area can be more accurately viewed. Fig. 4 shows the area under the ⟨220⟩ cuprite reflection, typical of all the reflections, plotted against time.

Peak area values from the water droplet increase steadily from time = 0 s, showing slow conversion to cuprite. Some cuprite is present from the start either from patina preparation, or exposure to moisture at some point between preparation and testing. From a video taken during measurement visible cuprite formation (cuprite is red–brown) does not occur until t = 43 min, but the plot in Fig. 4 shows that its formation commences immediately on contact with water. This perhaps suggests that cuprite formation occurs below the surface (perhaps at the nantokite-copper interface), but within the interaction volume of SR-X-rays so it not visible to the naked eye.

The cuprite peak area increases sharply at approximately t = 43 min in the 1% sodium sesquicarbonate droplet. A video taken during this experiment shows that t = 43 min corresponds to the start of growth of a bright orange layer on the surface of the coupon from the coupon edge (see Supplementary Information). Corrosion starts from an irregularity where the coupon was cut from a sheet. Sodium sesquicarbonate is in fact used as an active conservation treatment for chloride-infected metals [18,19]. It transforms nantokite to cuprite, therefore 'removing' chlorides from the copper artefact. The final peak area of cuprite is greater for the sesquicarbonate droplet, thus showing the effectiveness of this system as a conservation treatment for the removal of chlorides.

After the droplet experiment was completed in DI water, the nantokite conversion to cuprite was forced to completion by soaking the coupon in 50 mL water for 3 h. The result was complete conversion to cuprite (Fig. 5). The presence of a large volume water ensures the pH does not fall under pH 5.2, thus allowing complete conversion from nantokite to cuprite. Despite this result, it is possible (given more experiment time) that on exposure to ambient conditions prior to soaking the cuprite could have eventually progressed to trihydroxychlorides (via nantokite) if chloride ions remained in the material. Moreover the copper peak intensity increases substantially after soaking, which means that the resulting cuprite layer is thinner than the initial nantokite. This decrease in thickness could be due to the removal of chlorides into aqueous solution.

4. Conclusion

A nantokite patina was exposed to a 50 μL droplet of DI water or, in a separate experiment, 1% sodium sesquicarbonate. An increase in cuprite peak area was measured over time showing the reaction of nantokite with water to produce cuprite under these conditions. Although full conversion to cuprite did not occur, the process was more complete for the sesquicarbonate exposure. Soaking the coupon in water after the droplet experiment caused full transformation from nantokite to cuprite. In conclusion, the

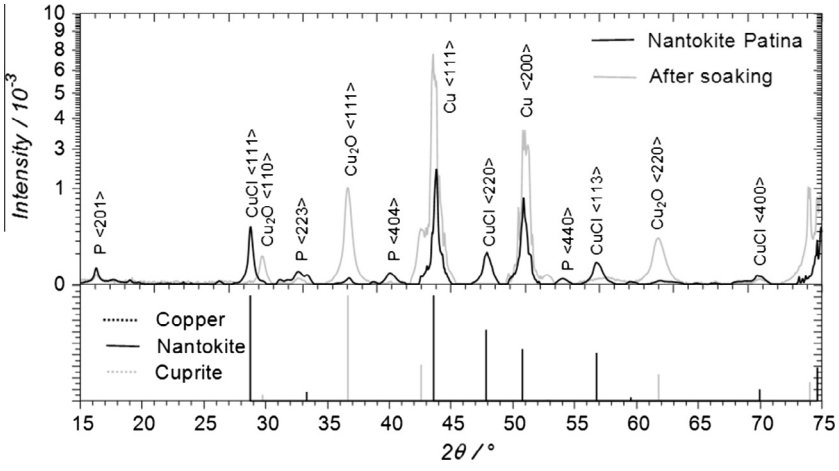

Fig. 5. SR-XRD pattern after soaking in DI water. Note the use of a square root scale for the intensity to show low intensity peaks.

Please cite this article in press as: R. Grayburn et al., Tracking the progression of bronze disease – A synchrotron X-ray diffraction study of nantokite hydrolysis, Corros. Sci. (2014), http://dx.doi.org/10.1016/j.corsci.2014.11.021

reaction of nantokite to cuprite is slow but can be completed over time and with bulk water, simulating burial or conservation conditions. In relation to the possible paths bronze disease could take, it seems it would depend on concentration of water available. If there is an excess of water, nantokite reacts to form cuprite whereas in a more oxygen rich environment nantokite prefers to form paratacamite [13].

Acknowledgements

esaProject and the eCell design are copyright 2013 Dowsett and Adriaens, and made available by EVA Surface Analysis. Also support from the Fund for Scientific Research – Flanders (FWO) is gratefully acknowledged. In addition, the ESPRC is thanked for the scholarship of M. Hand. The universities of Warwick (Physics department) and Ghent (BoF) are thanked for the funding of R. Grayburn.

Appendix A. Supplementary material

Supplementary data associated with this article can be found, in the online version, at http://dx.doi.org/10.1016/j.corsci.2014.11.021.

References

[1] D. Scott, Copper and Bronze in Art: Corrosion, Colorants, Conservation, Getty Publications, berlin, 2002.
[2] a.M. Alfantazi, T.M. Ahmed, D. Tromans, Corrosion behavior of copper alloys in chloride media, Mater. Des. 30 (2009) 2425–2430.
[3] L. Robbiola, J. Blengino, C. Fiaud, Morphology and mechanisms of formation of natural patinas on archaeological Cu–Sn alloys, Corros. Sci. 40 (1998) 2083–2111.
[4] G. Kear, B.D. Barker, F.C. Walsh, Electrochemical corrosion of unalloyed copper in chloride media––a critical review, Corros. Sci. 46 (2004) 109–135.
[5] M. Chmielová, J. Seidlerová, Z. Weiss, X-ray diffraction phase analysis of crystalline copper corrosion products after treatment in different chloride solutions, Corros. Sci. 45 (2003) 883–889.
[6] J. Wang, C. Xu, G. Lv, Formation processes of CuCl and regenerated Cu crystals on bronze surfaces in neutral and acidic media, Appl. Surf. Sci. 252 (2006) 6294–6303.
[7] D.A. Scott, Bronze disease: a review of some chemical problems and the role of relative humidity, J. Am. Inst. Conserv. 29 (1990) 193–206.
[8] A. Doménech-Carbó, M.T. Doménech-Carbó, V. Costa, Electrochemical basis of corrosion of cultural objects, in: A. Doménech-Carbó, M.T. Doménech-Carbó, V. Costa (Eds.), Electrochemical Methods in Archaeometry, Conservation and Restoration, Springer Berlin Heidelberg, Berlin, Heidelberg, 2009, pp. 123–134.
[9] I.D. Macleod, Bronze disease: an electrochemical explanation, Bull. ICCM 7 (1981) 16–26.
[10] D.A. Scott, A review of copper chlorides and related salts in bronze corrosion and as painting pigments, Stud. Conserv. 45 (2000) 39–53.
[11] NIST, Standard Reference Data Program, Boulder, Colorado, 2011.
[12] G. Bianchi, P. Longhi, Copper in sea-water, potential-pH diagrams, Corros. Sci. 13 (1973) 853–864.
[13] A.A.M. Pollard, R. Thomas, P. Williams, T. Drayman-Weisser, The copper(II) chloride system and corrosion: a complex interplay of kinetic and thermodynamic factors, in: Terry Drayman-Weisser (Ed.), The Conservation of Bronze Sculpture in the Outdoor Environment: A Dialogue among Conservators, Curators, Environmental Scientists, and Corrosion Engineers, National Association of Corrosion Engineers, Houston, Texas, United States, 1983, pp. 123–133.
[14] M. Dowsett, A. Adriaens, C. Martin, L. Bouchenoire, The use of synchrotron X-rays to observe copper corrosion in real time, Anal. Chem. 84 (2012) 4866–4872.
[15] A. Adriaens, M. Dowsett, K. Leyssens, B. Van Gasse, Insights into electrolytic stabilization with weak polarization as treatment for archaeological copper objects, Anal. Bioanal. Chem. 387 (2007) 861–868.
[16] R.B. Faltermeier, A corrosion inhibitor test for copper-based artifacts, Stud. Conserv. 44 (1998) 121–128.
[17] M.G. Dowsett, A. Adriaens, Cell for simultaneous synchrotron radiation X-ray and electrochemical corrosion measurements on cultural heritage metals and other materials, Anal. Chem. 78 (2006) 3360–3365.
[18] K. Leyssens, A. Adriaens, C. Degrigny, E. Pantos, Evaluation of corrosion potential measurements as a means to monitor the storage and stabilization processes of archaeological copper-based artifacts, Anal. Chem. 78 (2006) 2794–2801.
[19] M.G. Dowsett, A. Adriaens, G.K.C. Jones, N. Poolton, S. Fiddy, S. Nikitenko, Optically detected X-ray absorption spectroscopy measurements as a means of monitoring corrosion layers on copper, Anal. Chem. 80 (2008) 8717–8724.